

Proton-Proton Scattering at 437 Mev*

R. B. SUTTON, T. H. FIELDS, J. G. FOX, J. A. KANE, W. E. MOTT,† AND R. A. STALLWOOD
Carnegie Institute of Technology, Pittsburgh, Pennsylvania

(Received October 22, 1954)

This paper is a detailed account of measurements, already briefly reported, of the angular distribution of proton-proton scattering at 437 Mev. A description is given of the external proton beam: its collimation, angular spread, energy spectrum, and intensity. The counters, electronics, and targets are described. Two scattering arrangements were used. In one the polyethylene-carbon subtraction method with coincidence detection of the scattered and recoil protons was employed. In the other a counter telescope detected the protons emerging at a given angle from a liquid hydrogen target; at the larger angles but not at the smaller the scattered pairs could also be detected by coincidences between the telescope and another counter. At the smaller angles, when coincidence counting could not be used to insure detection of elastic p - p scattering, precautions were taken to absorb the particles produced in inelastic p - p collisions. The results are that the differential cross section for elastic proton-proton scattering rises smoothly from its value at 90° c.m. to a value about 20 percent higher at 17° c.m. The value at 90° c.m. is 3.49 ± 0.17 mb/sterad.

INTRODUCTION

THIS paper contains details of work, carried out at this laboratory and already briefly reported,^{1,2} on measurements of the angular distribution of elastic proton-proton scattering at 437 Mev.

Such measurements have been made by others for protons of energies up to 345 Mev.³ Descriptions of those for energies in the region 100 Mev to 345 Mev have also been published.⁴⁻¹⁰ These experiments indicate that, in this energy range, the nuclear differential scattering cross section in the c.m. system is approximately independent of angle and of energy.

Partial wave analyses of the scattering data for 240 Mev have been carried out recently.^{11,12} In these analyses at least S and P states of angular momentum must be included since an S -wave alone can hardly explain the magnitude of the cross section. Furthermore, recent experiments on the scattering of polarized protons by protons indicate that, in the energy region of 320 Mev and above, there are strong interactions in P and F states.¹³⁻¹⁵

It is of interest whether or not the p - p and n - p scattering cross sections are consistent with the hypothesis of charge independence. One of the requirements for this is that

$$\sigma_{p-p}(\theta=90^\circ) \leq 4\sigma_{n-p}(\theta=90^\circ),$$

where θ is the scattering angle in the c.m. system.¹⁶ Recent proton cross section measurements^{5,6} indicate that this inequality is satisfied for energies up to 350 Mev.

EXPERIMENTAL METHOD

I. Proton Beam

A. General Properties

The source of the high-energy protons was the Carnegie synchrocyclotron. A few percents of the beam is accelerated until it reaches a radius of about 70 inches ($n=1$), where it has sufficient energy to spiral out of the machine. At this radius the energy is about 450 Mev. These protons emerge with apparently equal intensity at all azimuths; their final path is tangent to a radius of about 83 inches. A collimator, appropriately inserted in the concrete shield wall, allows a small fraction of these protons to pass into the experimental region where the intensity is 2×10^6 cm⁻² sec⁻¹. The collimator restricts the beam to a size of $\frac{1}{2}$ in. \times $\frac{1}{2}$ in. The beam so obtained is quite monoenergetic and free from contamination. Figure 1 shows the cyclotron, the concrete shield wall, and proton collimator.

Figure 2 shows a considerably overexposed (1 min) x-ray film picture of the beam at the exit end of the collimator which is about 30 feet from the cyclotron. The target is normally placed 4 feet from the exit end of the collimator. The beam size at a distance of 20 feet from the collimator is 2.5 inches. This spreading is due

* Supported in part by the U. S. Atomic Energy Commission.

† Now at Gulf Research Laboratory, Harmorville, Pennsylvania.

¹ Mott, Sutton, Fox, and Kane, Phys. Rev. **90**, 712 (1953).

² Sutton, Fields, Fox, Kane, Mott, and Stallwood, Phys. Rev. **95**, 663 (1954).

³ Measurements have also been made at 429 Mev by Marshall, Marshall, and Nedzel [Phys. Rev. **92**, 834 (1953)], but these may have been affected by polarization of the incident beam to an extent which is under investigation [Phys. Rev. **93**, 1431 (1954)]. The value of the differential cross section at 90° c.m. would of course be unaffected by beam polarization.

⁴ Chamberlain, Segrè, and Wiegand, Phys. Rev. **83**, 923 (1951).

⁵ Marshall, Marshall, and Nedzel, Phys. Rev. **92**, 834 (1953).

⁶ Chamberlain, Pettengill, Segrè, and Wiegand, Phys. Rev. **93**, 1424 (1954).

⁷ O. A. Towler, Phys. Rev. **85**, 1024 (1952).

⁸ C. L. Oxley and R. D. Schamberger, Phys. Rev. **85**, 416 (1952).

⁹ Cassels, Pickavance, and Stafford, Proc. Roy. Soc. (London) **214**, 262 (1952).

¹⁰ Kruse, Teem, and Ramsey, Phys. Rev. **94**, 1795 (1954).

¹¹ A. Garren, Phys. Rev. **92**, 213 (1953).

¹² R. M. Thaler and J. Bengston, Phys. Rev. **93**, 643 (1954), and Thaler, Bengston, and Breit, Phys. Rev. **93**, 644 (1954).

¹³ Chamberlain, Segrè, Tripp, Wiegand, and Ypsilantis, Phys. Rev. **93**, 1430 (1954).

¹⁴ de Carvalho, Heiberg, Marshall, and Marshall, Phys. Rev. **94**, 1796 (1954).

¹⁵ Kane, Stallwood, Sutton, Fields, and Fox, Phys. Rev. **95**, 1694 (1954).

¹⁶ D. Feldman, Phys. Rev. **89**, 1159 (1953).

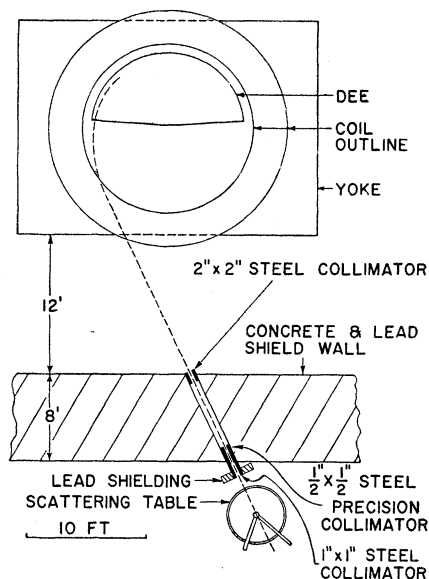


Fig. 1. Schematic diagram of cyclotron, shield wall, and external beam trajectory.

to the nature of the origin of the beam and to multiple scattering by the window on the cyclotron vacuum chamber and by air.

B. Energy

The energy and energy spread of the protons have been investigated three ways. The results are that most

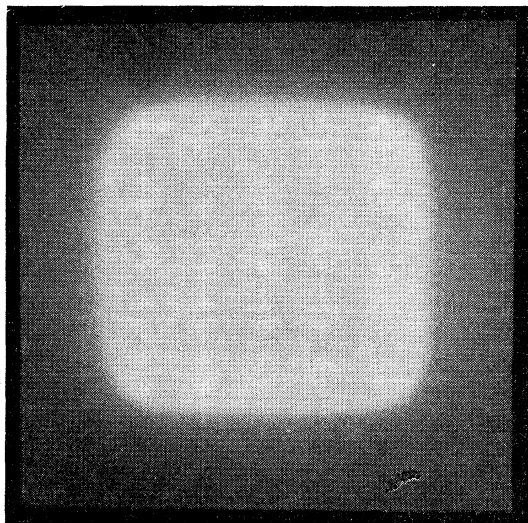


FIG. 2. A positive print from an x-ray film picture showing the cross section of the proton beam emerging from the collimator. The bright area was formed by the beam after emerging from the end of the $\frac{1}{2}$ inch by $\frac{1}{2}$ inch precision collimator which was 24 inches from the film. The sharp outer edges are the shadow of the 1-inch by 1-inch end-section of the collimator which shielded the counters from the spray of protons scattered by the walls of the precision collimator. The picture indicates the degree of alignment usually achieved.

of the protons at the target have an energy of 437 Mev which may vary by about 3 Mev due to variations in the magnetic field of the cyclotron. The instantaneous energy spread of these protons is probably less than 3 Mev. In addition, about 5 percent of the protons have energies between the maximum energy and 390 Mev. A negligible fraction have energy below 390 Mev. Those with energy lower than that of the main component probably suffered energy degradation in the collimator.

The first method used to investigate this problem was to count the number of coincidences between the scattered and recoil protons, in a p - p scattering experiment, as a function of angle between the two counters. For this experiment two stilbene scintillation counters were used. The stilbene crystals were 1 cm wide and 3.5 cm high in the plane perpendicular to the path of the detected protons and each was at a distance of 66 cm from the scattering target. The two counters were symmetrically placed with respect to the proton beam. The angle between the two counters was checked to about one minute by comparing the counting rates at angles where the slope of counting rate *versus* angle was steep, with and without interchanging the arms which supported the counters. The target was 0.54 g/cm^2 of CH_2 ; by replacing the CH_2 with C we were able to obtain the results, shown in Fig. 3, because of hydrogen scattering alone. Nonrelativistically the angle at the target between the two counters for peak intensity should of course be 90° . Relativistically this angle, 2θ , for symmetrically-placed counters, is given by

$$\tan 2\theta = \left(\frac{2m_0c^2}{E_0} + 1 \right) \tan \theta + \frac{2m_0c^2}{E_0} \cot \theta,$$

where E_0 is laboratory kinetic energy. For 437 Mev this angle is 84° . Thus from the counting rates at angles between 84° and 90° we could obtain an indication of the number of low-energy protons in the beam. An energy scale is included in Fig. 3. From the curve we were able to conclude that the peak lay at the correct angle within a maximum error of 10 minutes, that to an accuracy of 1 percent there were no protons with energies between 150 Mev and 350 Mev, and from consideration of the area and shape of the curve and the resolution of the equipment, that there may have been between 5 percent and 15 percent with energy above 350 Mev but below 437 Mev. This method, though it did not have very high dispersion, was used to obtain a semiquantitative result quickly and before we had set up better equipment for the purpose.

Higher dispersion was obtained by a method involving the observation of Čerenkov radiation. Plate glass of $\frac{1}{2}$ -inch thickness was placed in the proton beam. Čerenkov radiation from the glass passed through a lens and slit system and was detected by a 1P21 photomultiplier. The experimental arrangement is shown in Fig. 4. The intensity of the radiation was

measured as a function of its angle, θ , with the proton beam. The angle θ inside the glass is related to the $\beta (=v/c)$ of the protons by the relation $\cos\theta = 1/n\beta$, where n is the index of refraction of the glass. Hence, the radiation at a particular angle originates from protons of a particular β . The glass was rotated with the optical system so that the light detected always emerged perpendicular to the glass surface. Figure 5 shows the measured intensity of the radiation as a function of the angle θ ; an energy scale is also shown. The constant background appeared to be arising from fluorescence of the glass since it remained when the velocity of the protons was reduced by absorption in copper to a value at which Čerenkov radiation could not be emitted. A rough analysis of this curve indicated that about 5 percent—8 percent of the protons had energies between 390 Mev and the peak energy. The number of protons having energies between 300 Mev and 390 Mev was zero to an accuracy of 1 percent.

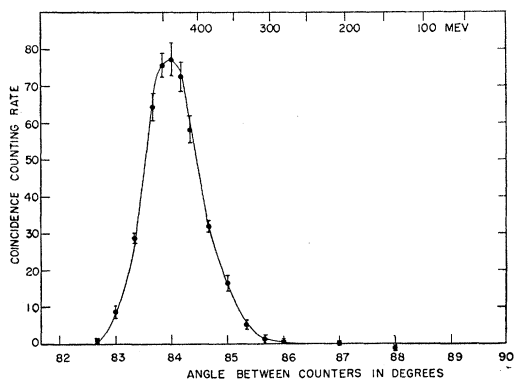


FIG. 3. p - p coincidence rate versus the angular separation between two counters which form equal angles with the incident beam. The width of the peak is largely due to the finite sizes of the counters. The energy scale shows the expected position of the peak for various incident proton energies.

Finally, having set up for other purposes a coincidence-anticoincidence counting telescope we have obtained differential range curves in copper for the protons. The telescope consisted of four scintillation counters as shown in Fig. 6; they are numbered 1, 2, 3, 4 in the order in which the beam traversed them. 1 and 2 are coupled in coincidence and used as a monitor; 1, 2, and 3 are in coincidence with 4 in anticoincidence. Thus, a count from $1+2+3-4$ arises from a particle traversing 1, 2, and 3, but not entering 4. The ratio of $1+2+3-4$ to $1+2$ as a function of copper thickness between 2 and 3 is shown in Fig. 7. The energies of protons at particular copper ranges are also shown. Because of nuclear absorption in the copper, there is a small counting rate of $1+2+3-4$. This rate varies slowly with thickness of copper, particularly in the first few centimeters because of the finite range of the fragments produced in nuclear events. At the end of the range of the protons the expected peak in counting rate is seen.

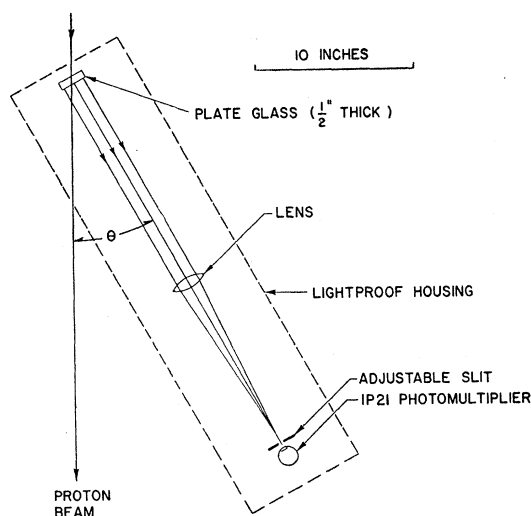


FIG. 4. Apparatus used to observe Čerenkov radiation.

Also shown for comparison is a differential range curve taken after the beam had passed through a magnet. The similarity of these curves at copper thickness below 1 inch indicates the absence of low-energy contamination even for energies below 150 Mev, a region not reached by the other methods described.

It would seem that the existing low-energy contamination should have little effect on the results of this experiment. The rate of loss of energy in argon is only 5 percent higher for 400 Mev than for 450-Mev protons. Hence, the effect on the chamber sensitivity is negligible. Since the scattering of protons is relatively insensitive to energy the cross sections should not be affected measurably.

C. Polarization

Since this beam spirals out of the cyclotron without being scattered there is no reason to expect it to be polarized. However, we have checked this point by

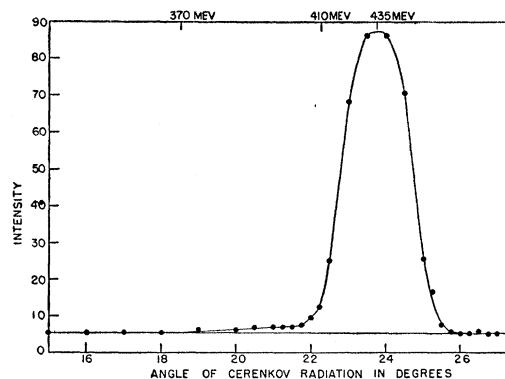


FIG. 5. Intensity of Čerenkov radiation produced by proton beam traversing glass as a function of the angle of emission. The beam direction was not measured accurately so that only relative angles are significant. The energy scale was computed so as to agree with the known energy of the beam.

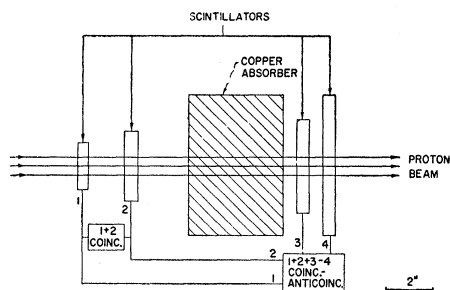


FIG. 6. Counter telescope used to obtain differential range curves.

scattering it from a carbon target and measuring the asymmetry of the scattered protons. Under conditions at which a 45 percent polarized beam gave an asymmetry of about 25 percent,¹⁵ the normal external beam gave (0.4 ± 0.7) percent. Furthermore, the p - p scattering data reported in this paper were taken on both sides of the beam. We thus conclude that these results are not subject to error on account of beam polarization.

D. Intensity Measurement

The method used to monitor the beam intensity was essentially that used by Chamberlain *et al.*⁴ The protons passed through an argon-filled ionization chamber which was very similar to the one used at Berkeley for the same purpose. A condenser of 0.181- μ f capacity was charged by the current from the chamber. The resulting condenser voltage was measured by a dc amplifier. The leakage resistance of the system was high enough to make loss of charge negligible during the charging time.

The ionization-chamber calibration is dependent upon a knowledge of the energy loss of protons in argon and the average energy loss per ion pair. These we have obtained from Aron *et al.*¹⁷ and Chamberlain *et al.*^{4,6}

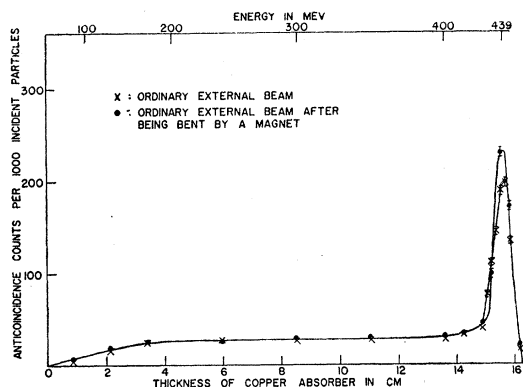


FIG. 7. Differential range curves. The copper absorber thickness and the energy scale have been corrected to allow for counter thicknesses.

¹⁷ Aron, Hoffman, and Williams, Atomic Energy Commission Report AECU-663, 1949 (unpublished) and W. Aron, University of California Radiation Laboratory Report UCRL-1325, 1951 (unpublished).

respectively. In the case of the energy loss per ion pair, we thus include the assumption that this quantity does not vary significantly from 345 Mev to 440 Mev.

II. Counters and Electronics

Scintillation counters were used to detect the scattered protons. They consisted of stilbene crystals or plastic scintillators viewed through short plastic light pipes by RCA-5819 photomultiplier tubes. The tubes were well shielded against stray magnetic fields. Signals were developed at the multiplier anodes across 100-ohm resistors. These signals were transmitted through about 100 feet of 100-ohm coaxial cable, RG7U, directly into a crystal diode coincidence circuit.¹⁸ The pulses were clipped to a duration of 2×10^{-9} sec by shorted cables of about 25 cm length connected at the coincidence input. The coincidence resolving time of the circuit was thus about 4×10^{-9} sec. The output pulses from the coincidence circuit were amplified by an Atomic 204-C linear amplifier. The pulses from the output of the amplifier discriminator were fed to a standard scaler. Coincidence counting rates were always sufficiently

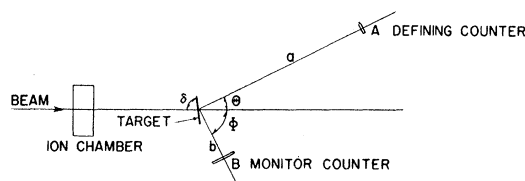


FIG. 8. The scattering arrangement used with CH_2 targets.

low that no dead time corrections were necessary. In order to obtain a pulse height spectrum of the coincidence pulses, the amplifier output was fed into a 24-channel pulse-height analyzer which was gated by the discriminator pulse.

III. Experiments Using a CH_2 Target

The experimental arrangement is shown in Fig. 8. Two counters *A* and *B* were so located and of such sizes that if counter *A* detected a proton scattered by hydrogen, *B* would detect the recoil proton. Counter *A*, which thus defined the solid angle, and which normally counted the high-energy proton, presented to the scattered protons an area of linear dimensions of the order of 2 to 3 cm. It was placed at a distance of about 1 meter from the target. Counter *B* was larger than *A* and nearer the target, its size and distance being determined by the requirements of geometry with allowance made for multiple scattering in the target. (*B* was sufficiently large that it would count the recoil even though either proton suffered a deviation in any direction of twice the root mean square multiple scattering angle calculated for complete traversal of the target.) In most cases the adequacy of the geometry

¹⁸ S. DeBenedetti and H. Richings, Rev. Sci. Inst. **23**, 37 (1952).

was checked by comparing results with B at two different distances.

Coincidence counts will arise from: (a) proton-proton scattering events from hydrogen, (b) quasi proton-proton scatterings from carbon in which an incident proton and a proton in the carbon nucleus are involved, (c) real coincidences which do not originate at the target, (d) accidental coincidences. In order to obtain the number of events (a), it is necessary to make a determination of (b), (c), and (d). At each angle it therefore becomes necessary to measure the coincidences, for a given number of incident protons, with a CH_2 target, a C target, and with no target, and to measure for each of these the accidental counts. Accidental counts were measured by increasing the length of cable connecting one counter to the coincidence circuit. The extra length was such that the time for transmission of a pulse along it was equal to the period of the radio-frequency voltage of the cyclotron. Thus the intensity of single counts was the same as when coincidence counting, but no true coincidences could be counted.

The carbon targets were chosen to have stopping power approximately equal to that of the corresponding CH_2 target. Thus, there were more carbon atoms per cm^2 of target surface than for the CH_2 targets. The reason for this choice was to have similar conditions for the CH_2 and C targets for emergence of very low-energy recoil protons from carbon.

If we use a CH_2 target with a surface density of carbon atoms equal to R times the surface density of the atoms in the carbon target, then the number of coincidences from hydrogen is given by

$$H = (\text{CH}_2 - \text{CH}_{2a}) - (B - B_a) - R[(C - C_a) - (B - B_a)].$$

Here CH_2 is the number of coincidences with the CH_2 target, CH_{2a} is the number of accidental coincidences with the CH_2 target, B and B_a , C and C_a are the corresponding quantities for no target and for the carbon target. Each of these quantities is measured for the same number of protons traversing the target.

In order to be certain that the discriminator was set low enough to trigger on all hydrogen coincidences, pulse height analyses of the coincidence pulses were made as described in Sec. II. A typical example of such a pulse height analysis is shown in Fig. 9, where the data using a carbon target and no target have been appropriately subtracted from the CH_2 data. These data were taken simultaneously with the recording of the coincidence counts. We concluded from curves such as this that the equipment was missing a negligible number of the proton-proton events.

It would be possible when making measurements at small scattering angles to count as true proton-proton scatterings the meson in counter B and the proton in counter A from the reaction

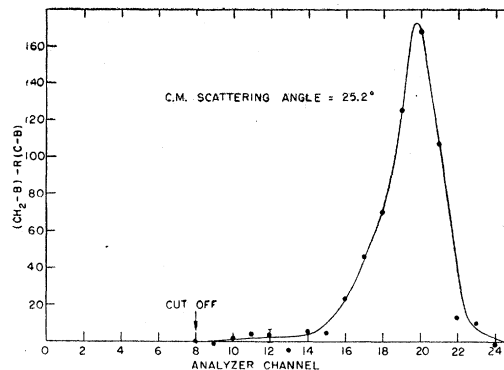
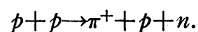


FIG. 9. Pulse height distribution of $p-p$ coincidence pulses in a typical run. The discriminator level was set at channel 8 as shown. The symbols C , R , B , and CH_2 are defined in the text.

The contribution of such events depends on the cross section for this reaction and on the angular correlation of the meson and proton. Because the range of the recoil proton when it appears at a large angle is very small compared to that of the meson in question, the coincidence-counting rate with 0.13 cm of copper in front of counter B should be due only to meson-proton coincidences. Such an experiment was carried out for the 25° center-of-mass measurement. It was found that the contribution to the measured scattering cross section from the meson production reaction was (0.5 ± 3) percent. It should also be noted that the counter geometry was always such that no events of the type $p + p \rightarrow \pi^+ + d$ could be counted.

IV. Experiments Using a Liquid Hydrogen Target

This method was used so that scattering at a smaller angle could be investigated (at center-of-mass angles less than 25° the lower energy proton of the pair has

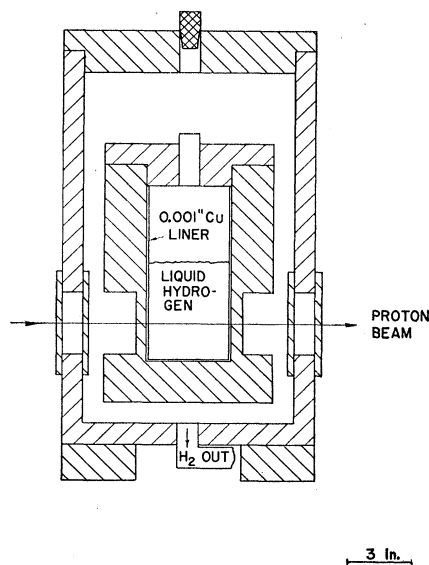


FIG. 10. Cross section of Styrofoam container for liquid hydrogen.

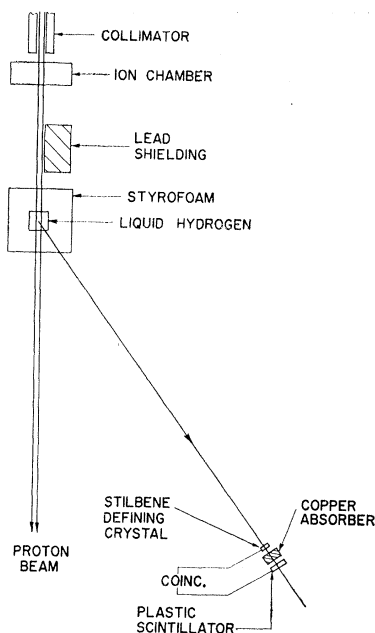


FIG. 11. The scattering arrangement used with liquid hydrogen. For the measurements at 90° c.m. and 50° c.m., an additional counter detected the other proton of the scattered pair in coincidence with the front telescope counter.

too low an energy to be counted with certainty) and also to provide a check on the work with CH₂ targets.

The target is shown in Fig. 10. It consisted of a double walled container made of Styrofoam. The liquid hydrogen was held in an inner container constructed of one-mil copper. This copper liner was used to prevent the hydrogen from coming in direct contact with the Styrofoam, and so producing thermal strains and, hence, possible cracking of the container; also, should a crack appear in a Styrofoam joint, the liner retains the hydrogen. The target was approximately 10 cm long in the beam direction. The hydrogen surface density was about twice that of the container. Warping of the copper while the container was being filled resulted in an uncertainty of about 5 percent in the surface density of the hydrogen. As a result the absolute cross sections obtained using liquid hydrogen have considerably greater errors than those from the CH₂ measurements. Thus, only relative cross sections are given for the liquid hydrogen data. The absolute value given is obtained only from CH₂.

Three methods were used to count protons scattered by the hydrogen: (1) At 90° and 50° c.m. scattering angle, both scattered protons were detected, as with

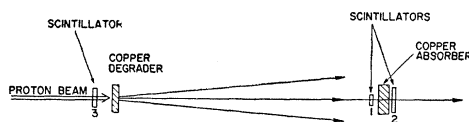


FIG. 12. Arrangement used for measuring the efficiency of the counter telescope as a function of the energy of the detected proton.

CH₂. Here a counter with a 10×15 cm plastic scintillator was used as counter *B*. (2) For all angles at which measurements were taken, a two-counter telescope was also used (Fig. 11) which detected only the high-energy proton of the pair. The front-telescope counter, which defined the solid angle, was a stilbene crystal and the back counter was of plastic and larger than the front one. At 90° and 50°, this telescope was used with no absorber between the two counters. (3) At 50 degrees 7.5 cm of copper, and at smaller angles 8.8 cm of copper, was inserted between the two counters of the above telescope. This copper stopped all particles accompanying meson production.

The measurements with no copper between the counters required a correction to be made for the mesons produced in some of the proton-proton collisions. These corrections were made on the basis of published cross sections^{19,20} for the reactions $p+p \rightarrow \pi^+ + d$ and

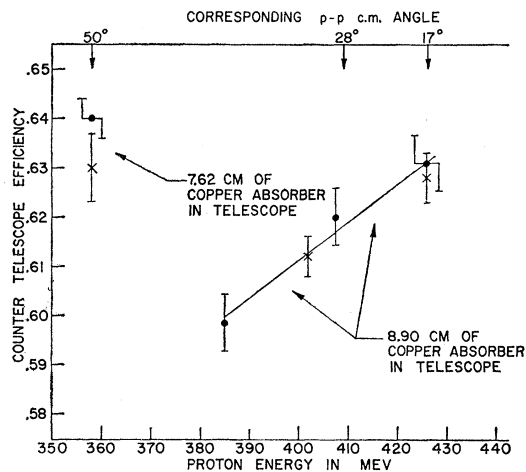


FIG. 13. Counter telescope efficiencies. The points marked with crosses were taken on a different day from those marked with circles, as described in the text. The various proton energies were obtained with various thicknesses of the copper degrader shown in Fig. 12.

$p+p \rightarrow \pi^+ + p + n$, and were about 5 percent of the measured scattering cross sections.

For the interpretation of the data taken with copper between the counters, it was necessary to calibrate the efficiency of the telescope for protons of the energy appropriate to each scattering angle. To determine the efficiency, the telescope was put in the direct proton beam at reduced intensity. Figure 12 shows the experimental arrangement. The required proton energy was obtained by degrading the beam with absorber. The efficiency of the telescope with copper between the counters was taken as the ratio of the telescope counts with copper to the counts with no copper for the same number of protons incident on the telescope. In order to monitor the protons incident on the telescope, a large

¹⁹ Fields, Fox, Kane, Stallwood, and Sutton, Phys. Rev. **95**, 638 (1954).

²⁰ A. H. Rosenfeld, Phys. Rev. **95**, 638 (1954).

TABLE I. Data obtained with CH₂ targets.

C.m. angle (deg)	$d\sigma/d\Omega$ (mb/sterad)	Standard deviation (mb/sterad)	Target thickness ^b (g/cm ²)	Target angle, δ (deg)	Counter sizes ^a		Counter distances (cm)		Counts per 10 ⁹ incident protons			Time in sec for 10 ⁹ incident protons
					A	B	A	B	CH ₂	C	B	
90	3.33	0.16	α	57.3	<i>a</i>	<i>b</i>	85	20	1303	193	0	3000
90	3.38	0.15	β	55.3	<i>c</i>	<i>b</i>	65	15	446	142	13	2100
90	3.58	0.17	β	55.0	<i>a</i>	<i>b</i>	65	15	706	212	33	2500
90	3.41	0.10	α	57.3	<i>a</i>	<i>b</i>	75	20	1736	284	30	3000
90 ^a	3.53	0.10	γ	70.0	<i>d</i>	<i>e</i>	80	30	156	24	6	180
90	3.49	0.18	γ	70.0	<i>d</i>	<i>e</i>	80	30	153	24	2	270
90	3.64	0.11	γ	70.0	<i>d</i>	<i>e</i>	80	20	172	41	8	170
65 ^d	3.62	0.15	β	45.3	<i>c</i>	<i>b</i>	75	20	265	52	5	2600
65 ^d	3.65	0.09	α	45.3	<i>a</i>	<i>b</i>	75	20	1590	287	24	1200
65 ^d	3.77	0.18	β	45.3	<i>a</i>	<i>b</i>	75	20	455	118	40	1000
65 ^d	3.42	0.13	α	41.5	<i>a</i>	<i>b</i>	100	20	926	189	29	1700
65 ^d	3.63	0.11	α	46.4	<i>a</i>	<i>b</i>	75	20	1520	232	11	2800
36 ^d	4.23	0.22	β	31.6	<i>a</i>	<i>b</i>	65	20	635	263	192	1000
36	4.02	0.15	γ	60.0	<i>c</i>	<i>b</i>	85	7	303	84	14	1300
36 ^d	4.22	0.17	β	33.9	<i>a</i>	<i>b</i>	65	20	432	75	19	2500
36 ^a	4.02	0.18	γ	47.0	<i>d</i>	<i>e</i>	130	12	139	33	6	250
36	4.06	0.14	γ	47.0	<i>d</i>	<i>e</i>	130	12	131	20	5	240
36	3.92	0.15	γ	47.0	<i>d</i>	<i>e</i>	130	18	122	13	5	160
30 ^a	3.96	0.14	γ	50.0	<i>d</i>	<i>e</i>	130	15	124	16	5	340
30 ^a	4.07	0.19	β	54.5	<i>d</i>	<i>e</i>	130	7.7	209	67	11	170
30	4.00	0.09	γ	54.5	<i>d</i>	<i>e</i>	130	15	115	12	2	130
30	4.10	0.13	γ	54.5	<i>d</i>	<i>e</i>	130	12	122	17	5	130
25	4.48	0.25	γ	60.0	<i>c</i>	<i>b</i>	85	5	384	139	29	1000
25 ^a	4.27	0.13	γ	50.0	<i>d</i>	<i>b</i>	130	10	138	20	5	170
25 ^a	4.36	0.18	γ	50.0	<i>d</i>	<i>b</i>	130	7.7	142	26	7	130

^a For these results accidental coincidences have been measured and included.
^b The symbols in this column have the following meaning: α —0.643 g/cm² CH₂, 0.781 g/cm² C; β —0.164 g/cm² CH₂, 0.223 g/cm² C; γ —0.110 g/cm² CH₂, 0.127 g/cm² C.
^c The symbols in this column have the following meaning: *a*—3.57 cm × 3.60 cm; *b*—3.50 cm × 3.52 cm; *c*—2.59 cm × 3.28 cm; *d*—2.06 cm × 3.97 cm; *e*—4.00 cm × 6.00 cm.
^d For these runs the defining counter detected the lower-energy proton.

third counter was placed next to the degrading absorber. Incident protons were measured by counting coincidences between this third counter and the front telescope counter. It was found that the distance between the telescope and the absorber used to degrade the beam energy, was large enough to have had no measurable effect on the efficiency measurement. Thus the efficiency was sufficiently independent of angular spread of the beam, and there was an negligible effect because of secondaries produced in the degrader. A check on the efficiency measurement was given by the comparison of the results at 50° obtained by the telescope method with those obtained by counting both protons.

Figure 13 shows the efficiency of the telescope as a function of proton energy. These data were taken immediately before the hydrogen runs. The two sets were taken with different counters, one set with sizes 2.5 × 3.5 cm and 10 × 10 cm, the other with sizes 3.5 × 3.5 cm and 7.5 cm diameter. The close agreement between these indicates that counter size relative to beam spread is unimportant when the second counter is large enough.

RESULTS

The results of the CH₂ experiments are given in Table I. Errors quoted are the standard deviations

obtained from the numbers of counts. For all angles except 25°, the correction due to the inclusion of the accidentals was one-half of one percent or less. At 25° the correction was less than 2 percent. Runs for which the times are over 1000 sec for 10⁹ incident protons are those for which the first results were published.¹

The results of the data obtained using the liquid hydrogen target are shown in Table II. Absolute values are not given because of the uncertainty in absolute length

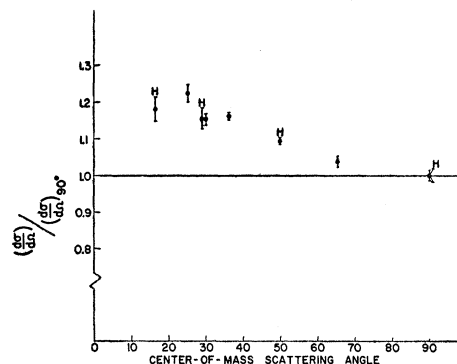


FIG. 14. The angular distribution of *p-p* scattering at 437 Mev. The points marked H were measured using a liquid hydrogen target; the other points were measured using a CH₂ target. The errors are standard deviations from counting statistics.

TABLE II. Data obtained with liquid hydrogen target.^a

C.m. angle (deg)	Method	$\frac{\sigma(\theta)}{\sigma(90^\circ)}$	Error	Telescope absorber (cm of copper)	Telescope efficiency	Dimensions of defining crystal	Distance of defining crystal (cm)	Ratio of H to empty target counting rate
90	Recoil	0.98	0.03	<i>f</i>	283	27
90	Telescope	1.04	0.04	0	1.00	<i>f</i>	283	1.5
90	Recoil	1.00	0.04	<i>b</i>	300	52
90	Telescope	1.00	0.05	0	1.00	<i>b</i>	300	3
50	Recoil	1.09	0.02	<i>f</i>	283	28
50	Telescope	1.11	0.03	7.62	0.63	<i>f</i>	283	5
50	Telescope	1.08	0.04	0	1.00	<i>f</i>	283	1.2
50	Recoil	1.11	0.02	<i>b</i>	300	50
50	Telescope	1.05	0.03	7.62	0.64	<i>b</i>	300	6.9
28	Telescope	1.17	0.05	8.90	0.62	<i>f</i>	283	2.7
28	Telescope	1.14	0.04	8.90	0.62	<i>b</i>	300	3.3
17	Telescope	1.19	0.05	8.90	0.63	<i>f</i>	283	0.75
17	Telescope	1.17	0.05	8.90	0.63	<i>b</i>	300	0.87

^a The methods in the second column are described in the text. The errors in the fourth column are standard deviations from counting statistics, including efficiency measurements. In the seventh column *f* denotes 2.50 cm × 3.47 cm; *b* denotes 3.50 cm × 3.52 cm.

of the target. The accidental counts here were completely negligible. The several runs at 90° and 50° show satisfactory agreement among the various methods used. The background became excessive at c.m. angles smaller than about 17° (7.5° lab angle).

The ratios of the average cross sections at the various angles relative to the average cross section at 90° for both the CH₂ and the liquid hydrogen data are given in Table III and Fig. 14. The agreement between the two sets of values is satisfactory.

A weighted average for the absolute cross section at 90° was obtained from the data in Table I. It is 3.49 mb/sterad with a standard deviation of 0.05 mb/sterad from counting statistics. We estimate a value of 5 percent for what might be termed the standard deviation of this cross section. It was obtained from an rms combination of the error from counting statistics and the estimated errors arising from multiple scattering, effective counter area and distance, target composition, angle, and thickness, properties of the dc-amplifier system which integrated the ion-chamber current, and background ionization in the chamber; also included was an estimated uncertainty of 2 percent in the value of the multiplication factor of the ionization chamber as given by the work at Berkeley.^{4,6,17}

TABLE III. Final average cross sections.

C.m. angle (deg)	$\frac{d\sigma/d\Omega}{d\sigma/d\Omega(90^\circ)}$	Statistical standard deviations
17	1.182	0.035
25	1.223	0.023
28	1.156	0.031
30	1.152	0.015
36	1.160	0.010
50	1.094	0.015
65	1.037	0.017
90	1.000	0.014

From the above angular distribution and absolute cross section at 90°, we calculate the total cross section for elastic nuclear *p-p* scattering at this energy to be 23.8 ± 1.2 mb.

DISCUSSION

As mentioned earlier, one of the main features of the angular distribution of proton-proton scattering in the range 150–345 Mev is its isotropy from 15° to 90° in the c.m. system within the experimental errors.²¹ The present results provide definite indications of a deviation from isotropy at 437 Mev in the form of a 20 percent rise in cross section at small angles. Hartzler and Siegel²² found similar behavior at energies in the neighborhood of 430 Mev; at 400 Mev and below their measurements were consistent with isotropy.

Our value of 3.49 ± 0.17 mb/sterad for the absolute cross section at 90° is related to the Berkeley values through the ionization-chamber calibration. Since our value is equal, within the errors, to theirs it appears that the cross section is quite constant from 120 Mev to 437 Mev. This conclusion is also supported by the results of Marshall, Marshall, and Nedzel.⁵ It is also of interest that their value for the 90° cross section of 3.42 ± 0.13 mb/sterad, which was obtained by direct counting of the incident flux, agrees excellently with our value.

A value of 1.5 mb/sterad for the *n-p* scattering cross section at 90° c.m. and a neutron energy of 400 Mev has been obtained by Hartzler and Siegel.²³ This value together with the present results indicates that the inequality

$$\sigma_{p-p}(\theta=90^\circ) \leq 4\sigma_{n-p}(\theta=90^\circ),$$

²¹ Kruse, Teem, and Ramsey (reference 10) have recently reported a 6 percent rise in $\sigma(\theta)$ from 90° c.m. to 40° c.m. at 97 Mev.

²² A. J. Hartzler and R. T. Siegel, Phys. Rev. 95, 185 (1954).

²³ Hartzler, Siegel, and Opitz, Phys. Rev. 95, 591 (1954).

discussed in the introduction, is satisfied in the 400-Mev region.

ACKNOWLEDGMENTS

It is a pleasure to thank Professor L. Wolfenstein for numerous valuable discussions on many aspects of

this problem. The help of Dr. S. A. Friedberg and other members of the Low Temperature Laboratory in providing liquid hydrogen is appreciated. The cooperation of the personnel of the Carnegie Institute of Technology Nuclear Research Center was an important contribution to the successful completion of this work.

Scattering of 151-Mev Positive Pions by Protons*

RAYMOND A. GRANDEY† AND ARNOLD F. CLARK‡
Carnegie Institute of Technology, Pittsburgh, Pennsylvania

(Received October 4, 1954)

Nuclear emulsions have been exposed to the external positive pion beam of the Carnegie synchrocyclotron and have been scanned for elastic $\pi-p$ scatterings. Seventy events have been found while scanning plates exposed to a final energy of 151 ± 7 Mev, which, combined with results obtained at Columbia and the recent accurate determinations of the total cross section in this region by the Carnegie Group, yield a value for the differential cross section of $d\sigma/d\Omega = (7.7 \pm 2.1) - (3.1 \pm 2.4) \cos\theta + (17.3 \pm 7.2) \cos^2\theta$ mb/sterad. The best Fermi type phase shifts calculated from the above are: $\alpha_3 = -26^\circ$, $\alpha_{33} = 50^\circ$, and $\alpha_{31} = 0^\circ$.

Recent data on pion-proton scattering at various energies are discussed, and it is found that the present data can be fitted with just three phase shifts which can be treated on semi-empirical models.

I. INTRODUCTION

THE elastic scattering of both positive and negative pions from hydrogen has been studied over a considerable range of energies. Counter techniques have been applied at Chicago, Columbia, and Rochester to obtain angular distributions for negative pion-proton scattering from 40 to 217 Mev.¹⁻⁶

Unfortunately, the very low positive-pion fluxes obtained externally from the present synchrocyclotrons have made it impractical to extend counter techniques in studying angular distributions for positive pion-proton scattering much above the 135-Mev point obtained by the Chicago group.¹ Nuclear emulsion techniques can be well applied in this high-energy positive-pion region. By using the hydrogen content of the emulsion as a scatterer, data can be collected with a minimum of cyclotron running time, and since the entire solid angle is available, this leads to the additional advantage of sampling scattering into all angles.

* This paper is a condensation of a thesis submitted by R. Grandey in partial fulfillment of the requirements for the degree of Doctor of Philosophy in Physics at Carnegie Institute of Technology. The research was partially supported by the U. S. Atomic Energy Commission. Preliminary results were reported in Phys. Rev. **94**, 766 (1954).

† U. S. Atomic Energy Commission Predoctoral Fellow.

‡ Now at the Radiation Laboratory, University of California, Livermore, California.

¹ Anderson, Fermi, Martin, and Nagle, Phys. Rev. **91**, 155 (1953).

² Fermi, Glicksman, Martin, and Nagle, Phys. Rev. **92**, 161 (1953).

³ M. Glicksman, Phys. Rev. **94**, 1335 (1954).

⁴ M. Glicksman, Phys. Rev. **95**, 1045 (1954).

⁵ Bodansky, Sachs, and Steinberger, Phys. Rev. **93**, 1367 (1954).

⁶ A. Roberts and J. Tinlot, Phys. Rev. **94**, 766 (1954).

II. EXPERIMENTAL PROCEDURE

A magnetically analyzed 160-Mev external positive-pion beam is available from the Carnegie cyclotron with a flux at the focus of the analyzing magnet of from 2 to 7 mesons per cm² per sec.⁷ This flux is so small that it causes serious experimental difficulties in a counter angular distribution experiment. The small flux requires exposures for plates on the order of one hour for intensities in the emulsion of 10⁴ mesons/cm².

The beam is formed by allowing the main internal proton beam to strike a Cu target placed at a cyclotron radius just inside the $n=0.2$ resonance. Positive pions produced in the backward direction are deflected out of the cyclotron by the fringing field and are focused at the same time.

The beam passes through a channel cut in the 8-ft thick magnetite concrete shield wall separating the cyclotron room from the experimental area and is further analyzed upon emergence by passing through a double-focusing 45° sector magnet. The energy and muon contamination of the beam were measured by taking range curves in Cu with counters. Three scintillation counters were placed before the absorber and one large counter behind. The ratio of quadruple to triple coincidences was counted as a function of absorber thickness. The equipment and geometry of the counter group⁷ was used. Figure 1 shows the range curve.

The relatively long exposure required together with

⁷ Ashkin, Blaser, Feiner, Gorman, and Stern, Phys. Rev. **96**, (1954).

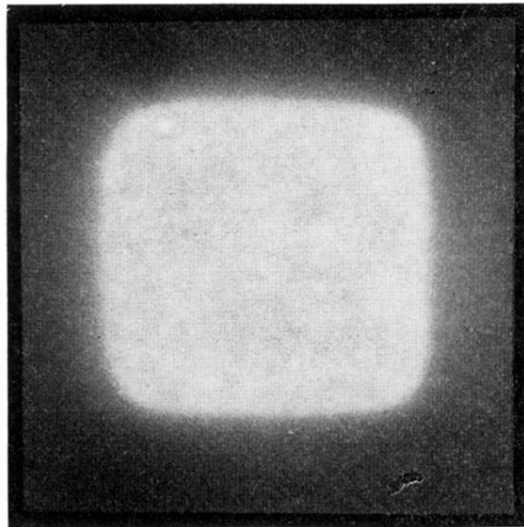


FIG. 2. A positive print from an x-ray film picture showing the cross section of the proton beam emerging from the collimator. The bright area was formed by the beam after emerging from the end of the $\frac{1}{2}$ inch by $\frac{1}{2}$ inch precision collimator which was 24 inches from the film. The sharp outer edges are the shadow of the 1-inch by 1-inch end-section of the collimator which shielded the counters from the spray of protons scattered by the walls of the precision collimator. The picture indicates the degree of alignment usually achieved.